The American Journal of Pathology, Vol. 183, No. 2, August 2013

The American Journal of PATHOLOGY

ajp.amjpathol.org

See related Commentary on page 330.

GROWTH FACTORS, CYTOKINES, AND CELL CYCLE MOLECULES

N,N-Dimethylacetamide Regulates the Proinflammatory Response Associated with Endotoxin and Prevents Preterm Birth

Sruthi Sundaram,* Charles R. Ashby Jr.,* Ryan Pekson,* Vaishali Sampat,* Ravikumar Sitapara,* Lin Mantell,* Chih-Hung Chen,* Haoting Yen,* Khushboo Abhichandani,* Swapna Munnangi,* Nikhil Khadtare,* Ralph A. Stephani,* and Sandra E. Reznik*†‡

From the Department of Pharmaceutical Sciences, St. John's University, Queens; and the Departments of Pathology† and Obstetrics and Gynecology and Women's Health,‡ Montefiore Medical Center, Albert Einstein College of Medicine, Bronx, New York*

CME Accreditation Statement: This activity ("ASIP 2013 AJP CME Program in Pathogenesis") has been planned and implemented in accordance with the Essential Areas and policies of the Accreditation Council for Continuing Medical Education (ACCME) through the joint sponsorship of the American Society for Clinical Pathology (ASCP) and the American Society for Investigative Pathology (ASIP). ASCP is accredited by the ACCME to provide continuing medical education for physicians.

The ASCP designates this journal-based CME activity ("ASIP 2013 AJP CME Program in Pathogenesis") for a maximum of 48 *AMA PRA Category 1 Credit(s)*™. Physicians should only claim credit commensurate with the extent of their participation in the activity.

CME Disclosures: The planning committee members and staff have no relevant financial relationships with commercial interests to disclose. The authors have no relevant financial relationship to disclose except for Charles R. Ashby, Jr., and Sandra E. Reznik who have filed a patent application for the use of DMA for inflammatory conditions (US patent application number 13/536,946).

Accepted for publication May 1, 2013.

Address correspondence to Sandra E. Reznik, M.D., Ph.D., Department of Pharmaceutical Sciences, St. John's University, 8000 Utopia Pkwy., St. Albert Hall G018-B, Queens, NY 11439. E-mail: rezniks@stjohns.edu.

The proinflammatory response leads to various types of pathologic pathways, including the development of preterm birth. Preterm birth occurs in 12% of deliveries in the United States and causes more than 70% of perinatal morbidity and mortality. The most common cause of spontaneous preterm birth is intrauterine infection in the mother. There is accumulating evidence indicating that the release of proinflammatory cytokines plays a critical role in the pathogenesis of inflammation-associated premature delivery. We found that the common organic solvent, *N,N*-dimethylacetamide (DMA), prevents endotoxin-induced preterm birth in timed pregnant C57BL/6 embryonic day (E)15.5 mice and rescues their pups from spontaneous abortion at doses many-fold lower than those currently used clinically and in a dose-dependent fashion. We also provide histologic evidence that DMA suppresses the endotoxin-triggered proinflammatory response by significantly attenuating inflammatory cell infiltration of placental tissue. Furthermore, immunoblotting analysis of placental tissue harvested from our murine models revealed DMA-mediated regulation of expression of the proinflammatory cytokines IL-1β, tumor necrosis factor α, and IL-6, and increased expression of the regulatory inflammatory cytokine IL-10. By using *in vitro* studies, we provide evidence that DMA suppresses macrophage function and that this small molecule prevents nuclear translocation of nuclear factor-kB. These results suggest that DMA represents a newly discovered, nontoxic therapy for a broad range of inflammatory disorders. *(Am J Pathol 2013, 183: 422–430; http://dx.doi.org/10.1016/j.ajpath.2013.05.006)*

A wide variety of disorders are associated with proinflammatory responses, including sepsis,[1] the fetal inflammatory response syndrome,[2] and preterm birth (PTB).[3] Premature delivery accounts for nearly half of long-term neurologic morbidity, and 60% to 80% of perinatal mortality, excluding infants with congenital anomalies,[3,4] and has increased in prevalence in the United States by 20% from 1990 to 2005. Unfortunately, there is no Food and Drug Administration–approved treatment for preterm labor and existing therapies are ineffective.[5]

Supported by NIH grants 1 K08 HD1209 (S.E.R.) and 1 R01 NS069577 (S.E.R. and R.A.S.).

C.R.A. and S.E.R. have filed a patent application for the use of DMA for inflammatory conditions (US patent application number 13/536,946).

http://dx.doi.org/10.1016/j.ajpath.2013.05.006

The release of proinflammatory cytokines plays a critical role in the pathogenesis of inflammation-associated premature delivery.[6,7] Bacteria in the gestational compartment of pregnant women have been shown to trigger the immune system via cell surface recognition molecules such as Toll-like receptor-2 and Toll-like receptor-4,[8,9] and T-helper cell (Th)1 cytokines such as IL-1β and tumor necrosis factor (TNF) α.[10–12] The inflammatory response is responsible for inducing steps in the latter part of the parturition cascade, such as decreased prostaglandin catabolism, functional progesterone withdrawal, increased expression of proteases, contraction-associated proteins, and increased uterine contractile activity.[13–15] Furthermore, inflammation can induce the rupture of membranes and cervical ripening, known to be mediated by matrix metalloproteinases (MMPs).[16] MMP-8 in particular has been used as a bedside test to identify patients at risk for imminent preterm birth.[17,18] Finally, Gomez et al[2] described the fetal inflammatory syndrome, which is characterized by increased fetal plasma IL-6 levels.

In a screen for nontoxic vehicles for ongoing studies, we discovered that *N*,*N*-dimethylacetamide (DMA) attenuates the excessive endotoxin-triggered proinflammatory response that leads to preterm delivery. DMA is an inexpensive, common aprotic organic solvent administered in a clinical setting at doses many-fold higher than those used in our experiments. In the current work, we present data from both *in vivo* and *in vitro* systems that uncovered DMA's potential as a novel anti-inflammatory agent.

Materials and Methods

Reagents

Lipopolysaccharide (LPS) (serotype 026:B6) and antibodies against TNF α, IL-6, IL-1β, MMP-8, and NF-kB p65 were purchased from Sigma-Aldrich (St. Louis, MO). IL-10 antibody was obtained from Epitomics (Burlingame, CA). RAW 264.7 cells were purchased from ATCC and cell culture media was obtained from Caisson Laboratories (North Logan, UT). Normal goat serum was purchased from Chemicon (Temecula, CA). Goat anti-rabbit secondary Alexa Fluor 595–conjugated antiserum was acquired from Molecular Probes (Eugene, OR). Lysis, loading, running, and transfer buffers, as well as molecular weight standards and polyvinylidene difluoride membranes were purchased from Life Technologies (Grand Island, NY). Skim milk powder and Bradford reagent were obtained from EMD Chemicals (Gibbstown, NJ). Anti-rabbit IgG, horseradish-peroxidase–linked whole antibody was purchased from GE Healthcare (Buckinghamshire, UK), and DAPI was purchased from Molecular Probes. Autoradiographic film was obtained from Denville Scientific (Metuchen, NJ). Stripping buffer was purchased from Thermo Scientific (Rockford, IL). The RNeasy Mini kit and RNAlater were purchased from Qiagen (Valencia, CA). Amino Allyl MessageAmp II aRNA (also called cRNA) amplification kits were purchased from Ambion (Austin, TX). Glyceraldehyde-3-phosphate dehydrogenase probes were purchased from Applied Biosystems/Life Technology (Carlsbad, CA). SYBR Green Master Mix was purchased from Qiagen. The Griess reagent kit was purchased from Promega (Madison, WI). DMA was purchased from Sigma-Aldrich. Purity of DMA was confirmed in one of our own laboratories by gas chromatography–mass spectroscopy. All other reagents were purchased from Sigma-Aldrich and VWR (Bridgeport, NJ).

Animals

Eight-week-old female C57Bl/6 mice were purchased from Taconic Laboratories (Hudson, NY). All procedures complied with the St. John's University Animal Care and Utilization Committee of the College of Pharmacy and Health Sciences. Research was conducted according to the NIH Guide for the Care and Use of Laboratory Animals, eighth edition, National Research Council (US) Committee for the Update of the Guide for the Care and Use of Laboratory Animals.

In Vivo Studies of the Effect of DMA on PTB

A total of 48 timed-pregnant mice weighing between 27 and 36 grams were given i.p. injections of 50 mg/kg LPS

Table 1 DMA Prevents LPS-Triggered PTB and Spontaneous Abortions in a Dose-Dependent Fashion

		DMA treatment, mg/kg					
Group	Control	0.2	0.39	0.78	1.56	3.1	Sham
Received 50 mg/kg LPS	Yes	Yes	Yes	Yes	Yes	Yes	No
Number of mice	9	7	8	10	6	8	4
Number of mice that delivered	8	5	3*	2†	0†	0‡	0
Number of pups	69	47	46	73	47	52	28
Number of pups spontaneously aborted	30	12†	5§	4§	0§	0§	0

Mice were treated with LPS followed by varying does of DMA, as indicated. Sham mice were injected with PBS in lieu of LPS. The proportion of LPS-induced mice delivering was decreased significantly at the four highest doses of DMA. The proportion of pups prematurely delivered and hence spontaneously aborted was reduced significantly at all five doses of DMA tested.

*$P < 0.05$.
†$P < 0.01$.
‡$P < 0.001$.
§$P < 0.0001$.

(serotype 026: B6; Sigma) dissolved in 500 μL PBS on E15.5 (t = 0 hours), following previously established protocols.[19–21] Mice then randomly were assigned to the control group or one of five treatment groups. At t = −0.5 hours and t = 10 hours they were injected with either 0.5 mL of PBS (control group) or 0.1 mL of increasing concentrations (6.25%, 12.5%, 25%, 50%, and 100%) of DMA (treatment groups). In addition, a sixth group of four animals (sham group) received an i.p. injection of 0.5 mL PBS in lieu of LPS and the PBS injections at −0.5 and t = 10 hours (Table 1). Mice were autopsied at 24 hours to confirm pregnancy, to determine the number of pups retained *in utero*, and to evaluate pups for congenital anomalies.

Histologic Analysis of the Effect of DMA on Inflammatory Cell Infiltration

Placentas were harvested during necropsy and fixed in 10% buffered formalin. Fixed tissues were paraffin-embedded, sectioned at 4 μm, and stained with H&E. All slides were examined by three blinded observers (K.A., S.M., and S.E.R.), one of whom is a practicing pathologist (S.E.R.), and graded for extent of inflammatory cell infiltration. The slides initially were scanned at ×100 magnification to identify any areas of active inflammation. The three most active (Invitrogen, Carlsbad, CA) fields at ×400 on each slide then were used for analysis. Slides with the three most active fields containing an average of 0 to 5 neutrophils were graded as 1, slides with the three fields containing an average of 6 to 50 neutrophils were graded as 2, and slides with the three most active fields containing greater than 50 neutrophils on average were graded as 3. The pathologist observer trained the nonpathologist observers before grading began and concordance among the three observers was confirmed with test slides. Sections were examined with a Nikon Eclipse 80i light microscope and images were captured with a Nikon Digital Sight camera (Nikon, Melville, NY).

cDNA Microarray Analysis

Five additional C57BL/6 timed-pregnant mice were induced with LPS and injected at E15.5 as described earlier. Twelve control E15.5 mice (distinct from mice used in the *in vivo* study) received a sham i.p. injection of PBS in lieu of LPS. Placentas were collected on E16.5, 24 hours after LPS injection or sham injection. Mice were sacrificed and rapidly hysterectomized. Placentas were placed immediately in RNAlater. Total RNA extraction was accomplished with an RNeasy Mini kit (Qiagen). Total RNA was quantified by measuring the absorbance at 260 nm (A_{260}). The purity of RNA was determined by measuring the A_{260}/A_{280} ratio. The ratio of A_{260} to A_{280} was within a range of 1.7 to 2.1 for all samples used for RNA amplification. RNA integrity was assessed by performing gel electrophoresis using 1.2% denatured agarose gels run at 100 volts (5 to 7 V/cm). Total RNA samples displaying two sharp (28S and 18S) rRNA bands were used for RNA amplification.

mRNA was extracted from samples of total RNA, amplified, and labeled by using the Amino Allyl MessageAmp II aRNA amplification kit (Ambion). Samples were quantified with a Nanodrop D1000 spectrophotometer (NanoDrop Technologies, Inc., Wilmington, DE). Poly(U) RNA (aRNA) also was subjected to gel electrophoresis and samples appearing as a smear from 6 to 0.5 kb were retested. An aliquot of 5 to 10 μg of each aRNA sample was lyophilized and then analyzed by a bioanalyzer (Agilent, Santa Clara, CA). Equimolar amounts of control samples were pooled and labeled with Cy3 (which fluoresces green), whereas samples from the five LPS-induced mice were labeled individually with Cy5 (which fluoresces red). Five hybridizations were performed. Each array was hybridized with the pooled control sample and a different Cy5-labeled sample.

Two color oligo arrays were designed and printed at the cDNA Microarray Facility of the Albert Einstein College of Medicine (Bronx, NY). Each array consists of 32,767 spots, which includes 192 sequences for quality control of the arrays, and represents the entire mouse genome. Arrays were prehybridized in preheated 35% formamide, 0.5% SDS, 2% salmon sperm DNA, and 4× sodium chloride-sodium phosphate-EDTA−2.5× Denhardt's solution (Sigma-Aldrich) for 1 hour at 50°C.

For hybridization, equimolar amounts of Cy3- and Cy5-labeled aRNA were combined. The volume was adjusted to 18.5 μL, and 1.0 μL of 20× blocking buffer (1 mg/mL polydA, 10 mg/mL tRNA, and 1 mg/mL human/mouse Cot1 DNA), and 40.5 μL hybridization solution (35% formamide, 0.5% SDS in 4× SSPE−2.5× Denhardt's) were added. Samples then were heated at 85°C to 94°C for 1 minute, vortexed, and centrifuged at 2,700 × *g* for 2 minutes. They were incubated at 50°C for 1 hour, and then centrifuged at 13,000 × *g* for 3 minutes. Each array then was covered with 58 μL of the supernatant from this last centrifugation of each aRNA sample and hybridized at 50°C for 20 hours.

After hybridization, arrays were washed at 25°C for 5 minutes in 600 mL 2× standard saline citrate/0.1% SDS, 0.2× standard saline citrate/0.1% SDS, and 0.2× standard saline citrate, and promptly dried and scanned, using the GenePix 4000A microarray scanner (Axon Instruments, Foster City, CA). The UHR Cy3 Cy5 images were acquired with GenePix Pro software version 6.0 (Axon Instruments).

Gel Electrophoresis

Placentas were homogenized in 0.3 mL ice-cold lysis buffer for 2 minutes every 15 minutes over the course of 2 hours. The homogenates were centrifuged at 10,000 × *g* for 5 minutes. The protein contents of the supernatants were determined using the Bradford assay with bovine serum albumin as the protein standard.

A volume corresponding to 30 μg protein of each supernatant was added to 3 μL NuPAGE LDS sample buffer

(4×) (Invitrogen) and 1 μL NuPAGE sample reducing agent (10×). Distilled water was added until a volume of 12 μL was reached, and the samples were reduced at 95°C for 5 minutes. Gel electrophoresis was performed in an XCell SureLock mini cell apparatus (Invitrogen) using 12-well NuPAGE Bis-Tris gel for protein separation. The gel was allowed to run for 45 minutes with 3-(N-morpholino) propane sulfonic acid running buffer. Proteins then were transferred to a polyvinylidene difluoride membrane.

Immunoblotting

The polyvinylidene difluoride membranes were wetted with Tris-buffered saline with 0.1% Tween-20, pH 7.8, for 10 minutes and then blocked with 5% skim milk powder in Tris-buffered saline with 0.1% Tween-20 solution for 2 hours. Next, the membranes were incubated with primary antibodies diluted in the blocker solution overnight at 4°C. They were washed with Tris-buffered saline with 0.1% Tween-20 three times at intervals of 15 minutes at room temperature. The membranes were incubated with a 1:1000 dilution of secondary antibody, anti-rabbit IgG, horseradish-peroxidase–linked whole antibody, in blocker solution at room temperature for 2 hours. The membranes were washed again with Tris-buffered saline with 0.1% Tween-20 three times for 15 minutes and treated with the ECL Plus Western blotting detection system (GE Healthcare, Piscataway, NJ). Chemifluorescence was detected by exposure to autoradiography film. The membranes were stripped at room temperature, incubated with anti–glyceraldehyde-3-phosphate dehydrogenase primary antibody (1:1000), and the steps described earlier were repeated. Band densities were quantified using ImageJ software (NIH, Bethesda, MD). The density values of housekeeping protein glyceraldehyde-3-phosphate dehydrogenase immunoblots were used for normalization.

Measurement of Nitric Oxide Production

Murine macrophage RAW264.7 cells were seeded in 6-well plates and treated with various concentrations of DMA. At 1 hour, cells were stimulated with 0.1 μg/mL LPS. Cell supernatants were collected at 24 hours and centrifuged at $1000 \times g$ for 10 minutes to remove floating cells. Nitric oxide production was determined by measuring nitrite concentration in the supernatant using the Griess reagent system (Promega) as described by the manufacturer. Briefly, 50 μL of the sample was reacted with 50 μL of sulfanilamide and 50 μL of 0.1% N-1 naphthyl ethylenediamine dihydrochloride solutions in water, each treatment lasted 10 minutes and was protected from light. Absorbance was read at 540 nm using the Opsys MR microplate reader (DYNEX technologies, Inc, Chantilly, VA).

Immunocytochemical Analysis of the Effect of DMA on NF-κB Translocation

RAW 264.7 cells were seeded in 12-well plates and were allowed to adhere overnight at 37°C. Cells were grown with or without 100 ng/mL LPS in the presence or absence of 0.01 or 1 μmol/L DMA for 2 hours. After treatments, cells were fixed with 2% phosphate-buffered formaldehyde (pH 7.4) for 15 minutes and washed three times with PBS. Cells then were permeabilized with 0.2% Triton X-100 and nonspecific binding sites were blocked with 10% normal goat serum for 20 minutes. This step was followed by washing the cells with 1% bovine serum albumin in PBS and incubation with anti–NF-κB p65 primary antibodies overnight at 4°C. Incubation with goat anti-rabbit IgG conjugated with Alexa Fluor 594 was performed for 1 hour. Normal blocking serum without primary antibody was used as a negative control. To visualize the nuclei, cells were counterstained with DAPI. Cells were examined under an immunofluorescence microscope (Nikon).

Testing the Effect of DMA on Cell Viability

To measure the effect of DMA on cell viability, RAW 264.7 cells were seeded in 48-well plates and were allowed to adhere overnight at 37°C. Cells were stimulated with 1 μg/mL LPS in the presence of a series of concentrations of DMA for 24 hours. Cells then were incubated with 0.5% MTT for 2 hours at 37°C. MTT then was removed and isopropanol was added to the wells to solubilize the formazan crystals for 15 minutes. The amount of MTT formazan product was determined by measuring the absorbance of the resulting purple solution at 570 nm using a microplate reader (Multiscan; Thermo Electron Corporation, Milford, MA).

Statistical Analysis

For *in vivo* studies, the effect of the various DMA doses on the percentage of mice experiencing preterm delivery was determined with the Fisher exact test. Similarly, the Fisher exact test as well as the chi-square analysis were used to evaluate the significance of the effect of the various DMA doses on the percentage of pups dropped. Differences in rates of PTB and rates of pups delivered over time were evaluated with the log-rank (Mantel-Cox) or Gehan-Breslow-Wilcoxon test. The *U*-test was used to evaluate differences in inflammatory cell infiltration in histologic sections. Differences in the mean expression of cytokine proteins as determined in immunoblots and differences in cell viability resulting from exposure to varying concentrations of DMA were evaluated with the Student's *t*-test. Results were considered significant for P values less than 0.05.

For microarray analysis, the background-subtracted signals were normalized with the locally weighted scatterplot smoothing algorithm using in-house Perl scripts and R statistical package (*http://www.r-project.org*). Missing and low-intensity signals (root mean square < 300) were excluded from the analysis. The means and SD of the signal intensity were calculated for each gene in every group. Only genes with signal variability of 30% (sigma/mean %) or less were considered in the analysis. Up-regulated and down-regulated genes were obtained from the tails of the log ratio distribution

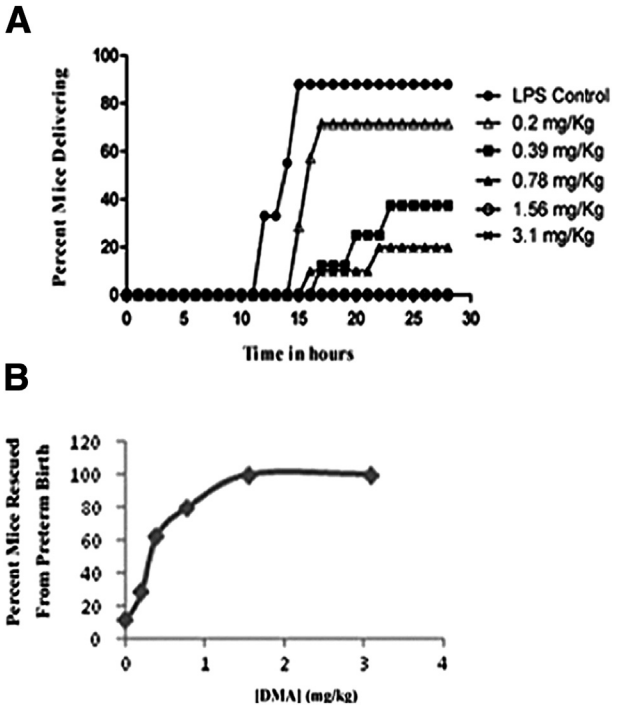

Figure 1 DMA prevents LPS-triggered PTB in a dose-dependent fashion. Mice given 50 mg/kg of LPS (i.p.) were treated with 3.1, 1.56, 0.78, 0.39, or 0.2 mg/kg DMA or PBS. All mice were observed for PTB for a period of 24 hours. **A:** The percentage of mice delivering at each dose of DMA over time. The percentage of mice delivering in the groups treated with varying doses (3.1, 1.56, 0.78, 0.39, and 0.2 mg/kg) of DMA were compared with the percentage of mice delivering in the control group ($P < 0.001$, $P < 0.01$, $P < 0.01$, $P < 0.05$, P = NS, respectively). **B:** The dose-response relationship between DMA and the prevention of PTB.

(3 sigma from the mean) ($P < 0.05$) and analyzed with Pathway Architect software (original version) (Stratagene, LaJolla, CA).

The effect of DMA on nitric oxide production in cultured RAW 264.7 cells was evaluated by analysis of variance.

Results

Among the eight mice responding to LPS, the mean time of delivery was 14.3 hours. At the two highest doses of DMA, 3.1 and 1.56 mg/kg, zero of eight and zero of six mice delivered, respectively. At a dose of 0.78 mg/kg, 2 of 10 (20%) mice delivered and the average time of delivery was 19.4 hours. At 0.39 mg/kg, 3 of 8 (37.5%) mice delivered, with 20.1 hours as the average time of delivery. At the lowest dose (0.2 mg/kg), 5 of 7 (71.43%) mice delivered and the average time of delivery was 16.1 hours (Table 1 and Figure 1A). A dose-dependent relationship between DMA and rescue of mice from PTB was observed (Figure 1B). Statistically significant differences in the percentage of mice delivering in the control group and in the groups treated with all of the doses of DMA except the lowest one were found, with rates of delivery decreasing as the dose of DMA was increased. Similarly, all but the lowest dose of DMA decreased the rate of premature delivery over time.

DMA also had a significant effect on the percentage of pups lost to spontaneous preterm delivery. Among the LPS-treated controls ($n = 69$ pups), 30 pups (43.5%) were lost secondary to preterm delivery. No pups were lost after treatment with 3.1 mg/kg DMA ($n = 52$) or with 1.56 mg/kg DMA ($n = 47$). After treatment with 0.78 mg/kg DMA, 4 of 73 (5.5%) pups were aborted spontaneously. At 0.39 mg/kg DMA, 5 of 46 (10.9%) pups were lost and 12 of 47 (25.5%) pups were dropped at 0.2 mg/kg (Table 1 and Figure 2A). Kaplan-Meier survival curves for rescued pups are shown in Figure 2B. A dose-dependent relationship between DMA and rescue of pups from spontaneous abortion was observed (Figure 2C). The number of pups spontaneously aborted in the DMA-treated groups was significantly lower than in the control group for all doses. All doses of DMA tested significantly decreased the rate of pups being delivered prematurely over time.

A total of 362 pups were examined in this study, and 265 of them were exposed to DMA. All pups were examined for abnormal numbers and positioning of extremities, abnormal craniofacial development, and abdominal wall defects. None of the mentioned anomalies was found. Moreover, no differences in gross appearance between pups born to DMA-treated versus DMA-untreated dams were identified.

Harvested placentas from mice subjected to sham injections ($n = 4$), LPS plus PBS ($n = 4$) and LPS plus DMA

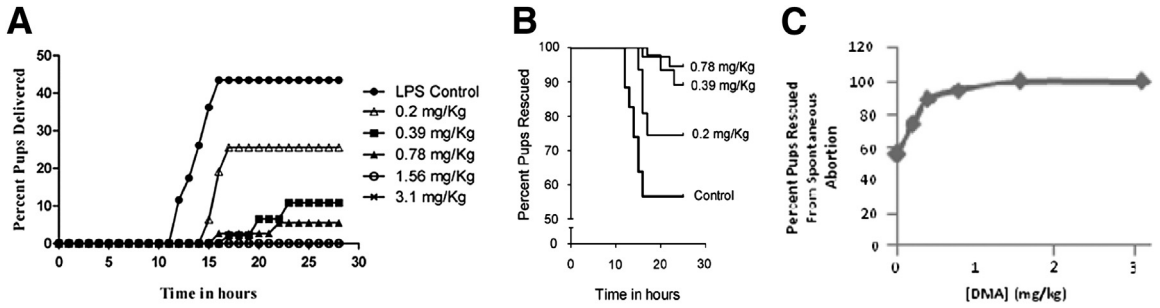

Figure 2 DMA rescues pups from LPS-triggered spontaneous abortion in a dose-dependent fashion. The cumulative percentage of pups lost to spontaneous abortions over time is shown (**A**) and the corresponding Kaplan-Meier survival curves are shown (**B**). The effect of varying doses of DMA on the rate of pups delivered over time was determined ($P < 0.0001$, $P < 0.0001$, $P < 0.0001$, $P < 0.0001$, and $P < 0.01$, corresponding to highest to lowest dose, respectively). **C:** The dose-response relationship between DMA and the rescue of pups from spontaneous abortion.

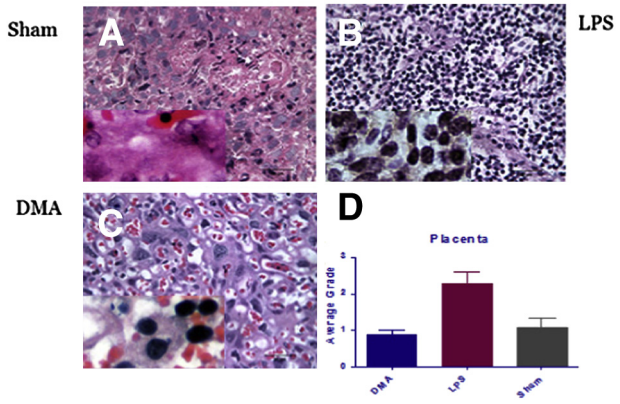

Figure 3 DMA suppresses recruitment of inflammatory cells to the placental labyrinth in LPS-treated mice. Placentas were harvested rapidly and fixed in 10% buffered formalin from three different groups of animals: sham control mice treated with PBS only ($n = 4$) (**A**), mice treated with LPS and PBS ($n = 4$) (**B**), and mice treated with LPS and 1.56 mg/kg DMA ($n = 4$) (**C**). For histologic analysis, fixed tissues were dehydrated and paraffin embedded, sectioned at 4 μm, and stained with H&E. Inflammatory cell infiltrates were graded as described. Numbers of polymorphonuclear neutrophils in sections of mouse placental labyrinth tissue from mice treated with LPS were compared with those in sham controls treated with PBS only ($P < 0.01$) and with those from mice rescued from LPS-induced PTB with 1.56 mg/kg DMA ($P < 0.01$) (**D**). **Insets**: Higher magnification (×600), showing increased number of inflammatory cells in LPS-stimulated tissue (**B** compared to **A**) and relatively decreased number of inflammatory cells resulting from treatment with DMA (**C** compared to **B**).

($n = 4$), showed vastly different degrees of labyrinthine inflammatory cell recruitment. Figure 3C shows a representative microscopic section of placental labyrinth collected from a mouse treated with LPS, but then rescued from preterm delivery with 1.56 mg/kg DMA. Inflammatory cells are rare. In fact, the histopathologic picture is similar to the representative micrograph produced with a placenta removed from a sham-injected mouse treated with only PBS (Figure 3A). A representative section from a mouse that developed preterm labor and delivery subsequent to treatment with LPS, in contrast, shows a dense collection of polymorphonuclear neutrophils (Figure 3B), obliterating the normal labyrinthine architecture. The results of a graded quantitative analysis performed by three blinded observers (K.A., S.M., and S.E.R.), including a placental pathologist (S.E.R.), are shown in Figure 3D. The increase in the number of inflammatory cells in placentas from LPS plus PBS-treated mice as compared with sham animals is statistically significant ($P < 0.01$). Similarly, the reduction in the number of leukocytes in placentas from mice treated with LPS, but ultimately rescued from PTB with DMA, as compared with mice induced to labor with LPS, was highly significant ($P < 0.01$).

Microarray analysis of mRNA from placental labyrinthine tissue harvested from mice induced to labor with LPS as compared with sham controls revealed activation of a network of inflammatory cytokines centered on IL-1β (Supplemental Table S1 and Supplemental Figure S1). Microarray data were deposited in Gene Express Omnibus (*http://www.ncbi.nlm.nih.gov/geo*; accession number pending). From these investigations of global differential gene expression, IL-1β, TNF α, IL-6, and IL-10 were selected for testing for changes in expression at the protein level resulting from DMA rescue from LPS-induced PTB.

As compared with placentas from mice that developed LPS-triggered PTB, placentas from DMA rescued mice had significantly reduced expression of IL-1β, TNF α, and IL-6 (Figure 4A). We hypothesized that DMA attenuated LPS-induced changes in the uterine cervix extracellular matrix that accompany labor. Levels of MMP-8 in placental tissue extracts from mice rescued from preterm birth with DMA were reduced in comparison with MMP-8 levels in mice that developed preterm delivery (Figure 4B). Importantly, IL-10 expression increased significantly more in placental tissue harvested from mice rescued from PTB with DMA as compared with control mice induced to labor with LPS (Figure 4C).

Next, we investigated whether the anti-inflammatory properties of DMA we had observed *in vivo* could be attributed to the effect of this compound on macrophages. We showed that DMA suppresses macrophage bactericidal activity in the presence of LPS stimulation in cultured RAW 264.7 cells (Figure 5). LPS stimulation in RAW 264.7

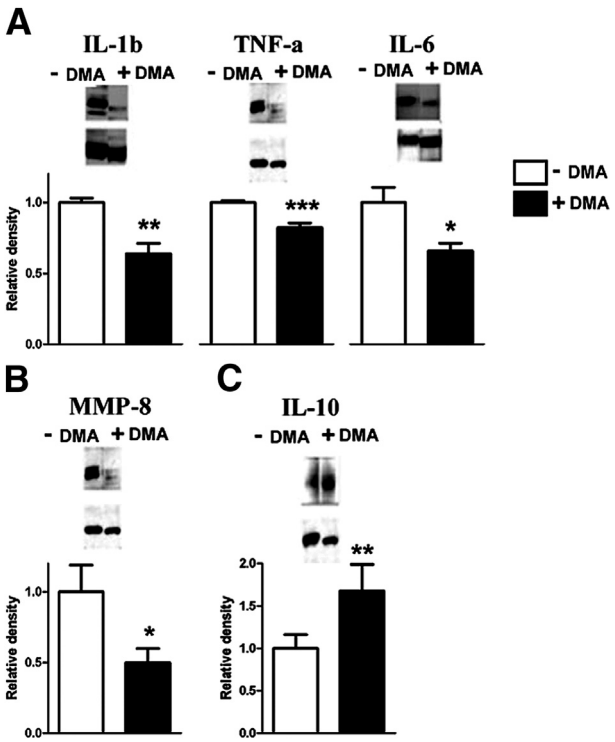

Figure 4 DMA suppresses expression of placental inflammatory signaling molecules in LPS-treated mice. Placental tissue lysates from LPS-induced mice ($n = 4$) and LPS-treated mice rescued from PTB with 1.56 mg/kg DMA ($n = 4$) were subjected to gel electrophoresis and immunoblotting. Band densities from control mice induced to PTB were normalized to 1.0 and compared with band densities from rescued mice after probing Western blots with antibodies directed against IL-1β ($P < 0.01$), TNF α ($P < 0.001$), and IL-6 ($P < 0.05$) (**A**); MMP-8 ($P < 0.05$) (**B**), and IL-10 ($P < 0.001$) (**C**). Glyceraldehyde-3-phosphate dehydrogenase was used for gel loading controls (lower bands). $^*P < 0.05$, $^{**}P < 0.01$, and $^{***}P < 0.001$.

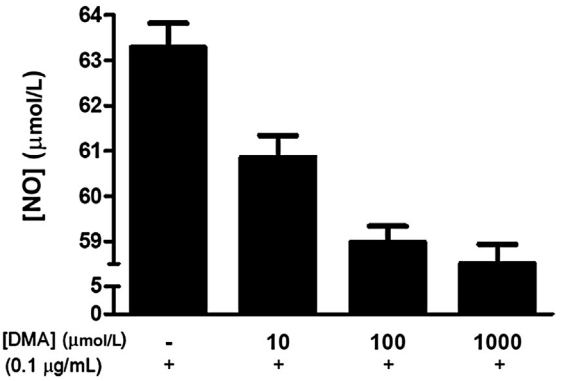

Figure 5 DMA suppresses nitric oxide (NO) synthesis in endotoxin-stimulated macrophages. RAW 264.7 cells were seeded in six-well plates in the absence or presence of a series of DMA concentrations and LPS. Nitric oxide production was measured using a Griess reagent kit, following the manufacturer's instructions. Analysis of variance showed a significant effect of DMA on macrophage function ($P < 0.0001$).

cells induced activation of the NF-kB signaling pathway, which is critical in cytokine release.[22] Figure 6 shows that immunoreactivity for the p65 unit of NF-kB in untreated cells was localized primarily in the cytoplasm, as indicated by a prominent red stain and a distinct hollow in the nucleus. However, treatment with LPS led to translocation of NF-kB into the nucleus (Figure 6). LPS-stimulated cells treated with DMA at concentrations of 0.01 μmol/L and 1 μmol/L displayed significantly reduced nuclear staining in comparison with cells treated with LPS alone, with greater inhibition of NF-kB translocation into the nucleus with a higher concentration of DMA (Figure 6). To confirm that DMA did not affect cell viability at the concentrations we used, cells also were grown in the absence or presence of LPS and treated with DMA concentrations ranging from 0.1 to 10 μmol/L. No significant effect on cell viability was detected at any of these concentrations (Supplemental Figure S2).

Discussion

The data presented indicate that DMA significantly attenuates the proinflammatory response mediated by LPS in timed-pregnant E15.5 mice. In the histologic analysis of placental labyrinthine tissues, DMA abolished the robust inflammatory cell infiltrate triggered by LPS. Immunoblotting analysis revealed that expression levels of the proinflammatory cytokines IL-1β, TNF α, and IL-6 in placentas from LPS-induced mice are decreased significantly by DMA. Moreover, DMA increased expression of the anti-inflammatory mediator, IL-10. Finally, DMA suppressed nitric oxide production and nuclear translocation of NF-κB in cultured macrophages.

DMA currently is used as a cryopreservative for platelets[23] and a solvent for a novel antiretroviral agent.[24] DMA is metabolized first to monomethylacetamide and then demethylated further to acetamide. Although long-term exposure to acetamide has been shown to cause liver cancer in rats,[25] DMA is not carcinogenic. It does not affect P450-dependent monooxygenase or phase II enzyme activities and has no significant effect on liver mixed-function oxidase and cytochrome c reductase activities.[26] On the other hand, with prolonged exposure, DMA causes liver injury in humans.[27] Importantly, it has been reported that DMA, when used as a vehicle for intravenous busulfan, does not produce adverse effects in pediatric oncologic patients at doses many-fold higher than those shown to suppress inflammation in this study.[28]

At doses high enough to produce toxic effects in the mothers, DMA causes embryotoxicity in sensitive species, namely rabbits.[29] In rats, on the other hand, no observed adverse effects were seen in fetuses until exposure to inhaled amounts of DMA reached levels high enough to produce toxic effects in the mothers.[30] In this study, 265 pups were directly examined and not one showed evidence of congenital anomalies.

We used a combination of *in vivo* and *in vitro* approaches in the current study to test the efficacy of DMA as a tocolytic agent and to investigate its mechanism of action. Our well-established murine model of infection-associated birth[31–36] has the advantage of allowing tight experimental control. On the other hand, by injecting LPS i.p. we have simulated systemic infection, rather than ascending infection per se. In future work, it will be interesting to test whether similar results are obtained when LPS is administered in the uterine horn. Data from both our *in vivo* model and our *in vitro* experiments support our hypothesis that DMA's ability to prevent preterm birth results from its suppressive effect on the inflammatory cascade. We note with interest that in recent literature the widely used poly (ADP-ribose) polymerase inhibitor PJ-34 also been found to suppress

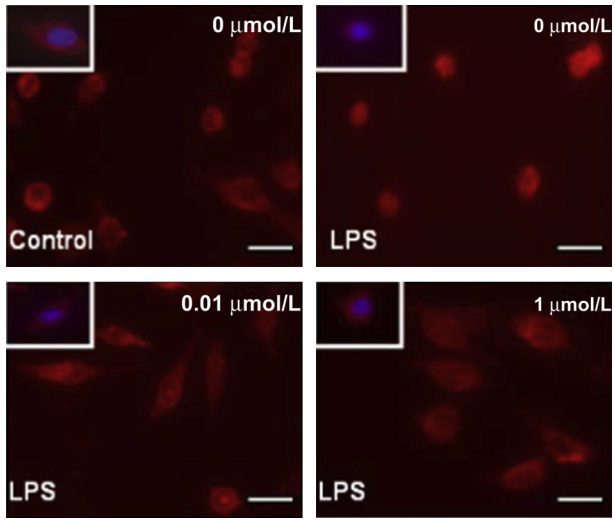

Figure 6 DMA inhibits nuclear translocation of NF-kB in endotoxin-stimulated macrophages. RAW 264.7 cells were seeded in 12-well plates with or without LPS for 24 hours in the absence or presence of DMA (concentration of DMA is indicated). Translocation of NF-kB was assessed by immunostaining the cells with anti—NF-kB antibody (red). DAPI stain was used to visualize nuclei (blue; **boxed areas**). Scale bars: 10 μm.

inflammation in various systems, including LPS-induced lung injury[37] and to inhibit NF-κB activation.[38] PJ-34 contains a DMA moiety; one might speculate whether the anti-inflammatory properties of the poly (ADP-ribose) polymerase inhibitor partially are explained by this aspect of its molecular structure.

A method of attenuating the excessive inflammatory response triggered by the Toll-like receptors represents a novel approach to the treatment of a variety of inflammatory disorders, including sepsis.[39,40] DMA has a clear therapeutic advantage over known anti-inflammatory agents, such as TNF α monoclonal antibodies and nitric oxide synthase inhibitors, which decrease the host's ability to fight off infections.[38] In fact, bacterial clearance is improved when overexuberant inflammation is held in check, as shown by the favorable effect obtained when Toll-like receptor−linked sphingosine kinase is inhibited.[41] Because inflammation is implicated in an extremely broad spectrum of disorders, including Alzheimer disease, cardiovascular disease, and diabetes mellitus,[42−55] the potential clinical impact of this molecule as an anti-inflammatory agent is striking.

Acknowledgments

We thank Helen Scaramell, Eileen Hussey, and the entire St. John's Animal Facility Staff for their assistance with maintaining and breeding the mice, Aldo Massini for his assistance with microarray analysis, and Ekatarina Milova for statistical analysis of the microarray data.

S.S. performed the *in vivo* and biochemical studies, contributed to the writing of the manuscript, the preparation of the figures, and the statistical analysis; C.A.R. conceived the original project from which this work arose; R.P. performed *in vitro* studies, the statistical analysis, and assisted with the preparation of the manuscript; V.S. and R.S. performed *in vitro* studies; L.M. conceived the *in vitro* studies and provided funding; C.-H.C. and H.Y. performed microarray studies; K.A. assisted with the *in vivo* experiments; S.M. assisted with the *in vivo* experiments and with the preparation of the manuscript; N.K. and R.A.S. supported the *in vivo* and *in vitro* experiments; and S.E.R. guided all aspects of the project, wrote the manuscript, and provided funding.

Supplemental Data

Supplemental material for this article can be found at *http://dx.doi.org/j.ajpath.2013.05.006*.

References

1. Janeway CA Jr, Medzhitov R: Innate immune recognition. Annu Rev Immunol 2002, 20:197−218
2. Gomez R, Romero R, Ghezzi, Yoon BH, Mazor M, Berry SM: The fetal inflammatory syndrome. Am J Obstet Gynecol 1998, 179: 194−202
3. Goldenberg RL, Culhane JF, Iams JD, Romero R: Epidemiology and causes of preterm birth. Lancet 2008, 371:75−84
4. Rush RW, Keirse MJ, Howat P, Baum JD, Anderson AB, Turnbull AC: Contribution of preterm delivery to perinatal mortality. Br Med J 1976, 2:965−968
5. Simhan HN, Caritis SN: Prevention of preterm delivery. N Engl J Med 2007, 357:477−487
6. Lappas M, Permezel M, Georgiou HM, Rice GE: Nuclear factor kappa B regulation of proinflammatory cytokines in human gestational tissues in vitro. Biol Reprod 2002, 67:668−673
7. Belt AR, Baldassare JJ, Molnár M, Romero R, Hertelendy F: The nuclear transcription factor NF-kappaB mediates interleukin-1beta-induced expression of cyclooxygenase-2 in human myometrial cells. Am J Obstet Gynecol 1999, 181:359−366
8. Elovitz MA, Wang Z, Chien EK, Rychlik DF, Phillipe M: A new model for inflammation-induced preterm birth: the role of platelet-activating factor and Toll-like receptor-4. Am J Pathol 2003, 163:2103−2111
9. Abrahams VM: Antagonizing toll-like receptors to prevent preterm labor. Reprod Sci 2008, 15:108−109
10. Romero R, Mazor M, Brandt F, Sepulveda W, Avila C, Cotton DB, Dinarello CA: Interleukin-1 alpha and interleukin-1 beta in preterm and term human parturition. Am J Reprod Immunol 1992, 27: 117−123
11. Romero R, Mazor M, Sepulveda W, Avila C, Copeland D, Williams J: Tumor necrosis factor in preterm and term labor. Am J Obstet Gynecol 1992, 166:1576−1587
12. Dudley DJ, Collmer D, Mitchell MD, Trautman MS: Inflammatory cytokine mRNA in human gestational tissues: implications for term and preterm labor. J Soc Gynecol Investig 1996, 3:328−335
13. Brown NL, Alvi SA, Elder MG, Bennett PR, Sullivan MH: Interleukin-1beta and bacterial endotoxin change the metabolism of prostaglandins E2 and F2alpha in intact term fetal membranes. Placenta 1998, 19:625−630
14. Challis JRG: Mechanism of parturition and preterm labor. Obstet Gynecol Surv 2000, 55:650−660
15. Hirsch E, Wang H: The molecular pathophysiology of bacterially induced preterm labor: insights from the murine model. J Soc Gynecol Investig 2005, 12:145−155
16. Cockle JV, Gopichandran N, Walker JJ, Levene MI, Orsi NM: Matrix metalloproteinases and their tissue inhibitors in preterm perinatal complications. Reprod Sci 2007, 14:629−645
17. Maymon E, Romero R, Pacora P, Gomez R, Athayde N, Edwin S, Yoon BH: Human neutrophil collagenase (matrix metalloproteinase 8) in parturition, premature rupture of the membranes, and intrauterine infection. Am J Obstet Gynecol 2000, 183:94−99
18. Nien JK, Yoon BH, Espinoza J, Kusanovic JP, Erez O, Soto E, Richani K, Gomez R, Hassan S, Mazor R, Edwin S, Bahado-Singh R, Romero R: A rapid MMP-8 bedside test for the detection of intra-amniotic inflammation identifies patients at risk for imminent preterm delivery. Am J Obstet Gynecol 2006, 195:1025−1030
19. Fidel PL, Romero R, Wolf N, Cutright J, Ramirez M, Araneda H, Cotton DB: Systemic and local cytokine profiles in endotoxin-induced preterm parturition in mice. Am J Obstet Gynecol 1994, 170:1467−1475
20. Hirsch E, Saotome I, Hirsh D: A model of intrauterine infection and preterm delivery in mice. Am J Obstet Gynecol 1995, 172:1598−1603
21. Kaga N, Katsuki Y, Obata M, Shibutani Y: Repeated administration of low-dose lipopolysaccharide induces preterm delivery in mice: a model for human preterm parturition and for assessment of the therapeutic ability of drugs against preterm delivery. Am J Obstet Gynecol 1996, 174:754−759
22. Ulloa L, Ochani M, Yang H, Tanovic M, Halperin D, Yang R, Czura CJ, Fink MP, Tracey KJ: Ethyl pyruvate prevents lethality in mice with established lethal sepsis and systemic inflammation. Proc Natl Acad Sci U S A 2002, 99:12351−12356
23. Odink J, Sprokholt R: Platelet preservation. I. The use of decrease in light absorbance as a screening method in cryopreservation studies on human platelets. Cryobiology 1977, 14:519−528

24. Aungst BJ, Nguyen NH, Bulgarelli JP, Oates-Lenz K: The influence of donor and reservoir additives on Caco-2 permeability and secretory transport of HIV protease inhibitors and other lipophilic compounds. Pharm Res 2000, 17:1175−1180
25. Kennedy GL Jr: Biological effects of acetamide, formamide, and their monomethyl and dimethyl derivatives. Crit Rev Toxicol 1986, 7: 129−182
26. Beyhl FE, Lindner E: Action of N, N-diethylacetamide on hepatic microsomal drug- metabolizing enzymes. Food Cosmet Toxicol 1981, 19:627−629
27. Jung SJ, Lee CY, Kim SA, Park KS, Ha BG, Kim J, Yu JY, Choi T: Dimethylacetamide-induced hepatic injuries among spandex fibre workers. Clin Toxicol (Phila) 2007, 45:435−439
28. Hempel G, Oechtering D, Lanvers-Kaminsky C, Klingebiel T, Vormoor J, Gruhn B, Boos J: Cytotoxicity of dimethylacetamide and pharmacokinetics in children receiving intravenous busulfan. J Clin Oncol 2007, 25:1772−1778
29. Stulla EF, Krauss WC: Embryotoxicity in rats and rabbits from cutaneous application of amide-type solvents and substituted ureas. Tox Appl Pharmacol 1977, 41:35−55
30. Okuda H, Takeuchi T, Senoh H, Arito H, Nagano K, Yamamoto S, Matsushima T: Developmental toxicity induced by inhalation exposure of pregnant rats to N,N-dimethylacetamide. J Occup Health 2006, 48:154−160
31. Koscica K, Sylvestre G, Reznik SE: The effect of phosphoramidon on inflammation-mediated preterm delivery in a mouse model. Am J Obstet Gynecol 2004, 190:528−531
32. Koscica K, Ananth CV, Placido J, Reznik SE: The effect of a matrix metalloproteinase inhibitor on inflammation-mediated preterm delivery. Am J Obstet Gynecol 2007, 196:551.e1−551.e3
33. Olgun N, Patel H, Wang W, Yen H, Stephani R, Reznik SE: The role of a 1,3,6- trisubstituted-2-carboxy-quinol-4-one, a novel putative selective ET_A antagonist, in controlling preterm labor in a mouse model. Can J Physiol Pharmacol 2008, 86:571−575
34. Wang W, Yen H, Chen C-H, Soni R, Jasani N, Sylvestre G, Reznik SE: The endothelin-converting enzyme-1 (ECE-1)/endothelin-1 (ET-1) pathway plays a critical role in infection-associated premature delivery in a mouse model. Am J Pathol 2008, 173:1−8
35. Wang W, Yen H, Chen C-H, Jasani N, Soni R, Koscica K, Reznik SE: Endothelin-1 and matrix metalloproteinase-1 function in the same molecular pathway in infection- associated preterm birth. Mol Med 2010, 16:505−512
36. Olgun NS, Stephani RA, Patel HJ, Reznik SE: Blockade of endothelin-1 with a novel series of 1,3,6-trisubstituted-2-carboxy-quinol-4-one's controls infection-associated preterm birth. Am J Pathol 2010, 177:1929−1935
37. Liaudet L, Pacher P, Mabley JG, Virág L, Soriano FG, Haskó G, Szabó C: Activation of poly(ADP-ribose) polymerase-1 is a central mechanism of lipopolysaccharide-induced acute lung inflammation. Am J Respir Crit Care Med 2002, 165:372−377
38. Zheng L, Szabo C, Kern TS: Poly(ADP-ribose) polymerase is involved in the development of diabetic retinopathy via regulation of nuclear factor-kappaB. Diabetes 2004, 53:2960−2967
39. Weighardt H, Holzmann B: Role of Toll-like receptor responses for sepsis pathogenesis. Immunobiology 2007, 212:715−722
40. Puneet P, Yap CT, Wong L, Lam Y, Koh DR, Moochhala S, Pfeilschifter P, Huwiler A, Melendez AJ: SphK1 regulates proinflammatory responses associated with endotoxin and polymicrobial sepsis. Science 2010, 328:1290−1294
41. Wadgaonkar R, Patel V, Grinkina N, Romano C, Liu J, Zhao Y, Sammani S, Garcia JG, Natarajan V: Differential regulation of sphingosine kinases 1 and 2 in lung injury. Am J Physiol Lung Cell Mol Physiol 2009, 296:L603−L613
42. Manduteanu I, Simionescu M: Inflammation in atherosclerosis: a cause or a result of a vascular disorder? J Cell Mol Med 2012, 16:1978−1990
43. Dowling JK, O'Neill LA: Biochemical regulation of the inflammasome. Crit Rev Biochem Mol Biol 2012, 47:424−443
44. Abbate A, Van Tassell BW, Biondi-Zoccai GG: Blocking interleukin-1 as a novel therapeutic strategy for secondary prevention of cardiovascular events. Biodrugs 2012, 26:217−233
45. Barber R: Inflammatory signaling in Alzheimer disease and depression. Cleveland Clin J Med 2011, 78(Suppl 1):S47−S49
46. Grishman EEK, White PC, Savani RC: Toll-like receptors, the NLRP3 inflammasome, and interleukin-1 in the development and progression of type 1 diabetes. Pediatr Res 2012, 71:626−632
47. Ma K, Jin X, Liang X, Zhao Q, Zhang X: Inflammatory mediators involved in the progression of the metabolic syndrome. Diabetes Metab Res Rev 2012, 28:388−394
48. Riccioni G, Back M: Leukotrienes as modifiers of preclinical atherosclerosis? Scientific World Journal 2012, 2012:490968
49. Ding HS, Yang J, Yang J, Ding JW, Chen P, Zhu P: Interleukin-17 contributes to cardiovascular diseases. Mol Biol Rep 2012, 39: 7473−7478
50. Romeo GR, Lee J, Shoelson SE: Metabolic syndrome, insulin resistance, and roles of inflammation—mechanisms and therapeutic targets. Arterioscler Thromb Vasc Biol 2012, 32:1771−1776
51. Calle MC, Fernandez ML: Inflammation and type 2 diabetes. Diabetes Metab 2012, 38:183−191
52. Gomez-Guerrero C, Mallavia B, Egido J: Targeting inflammation in cardiovascular diseases, still a neglected field? Cardiovasc Ther 2012, 30:e189−e197
53. Verri M, Pastoris O, Dossena M, Aquilani R, Guerriero F, Cuzzoni G, Venturini L, Ricevuti G, Bongiorno AI: Mitochondrial alterations, oxidative stress and neuroinflammation in Alzheimer's disease. Int J Immunopathol Pharmacol 2012, 25:345−353
54. Guergnon J, Combadiere C: Role of chemokines polymorphisms in diseases. Immunol Lett 2012, 145:15−22
55. Taube A, Schlich R, Sell H, Eckardt K, Eckel J: Inflammation and metabolic dysfunction: links to cardiovascular diseases. Am J Physiol Heart Circ Phys 2012, 302:H2148−H2165